*Research Article*

# Analysis of Human Electrocardiogram for Biometric Recognition

**Yongjin Wang, Foteini Agrafioti, Dimitrios Hatzinakos, and Konstantinos N. Plataniotis**

*The Edward S. Rogers Sr., Department of Electrical and Computer Engineering, University of Toronto,
10 King's College Road, Toronto, ON, Canada M5S 3G4*

Correspondence should be addressed to Yongjin Wang, ywang@comm.utoronto.ca

Security concerns increase as the technology for falsification advances. There are strong evidences that a difficult to falsify biometric trait, the human heartbeat, can be used for identity recognition. Existing solutions for biometric recognition from electrocardiogram (ECG) signals are based on temporal and amplitude distances between detected fiducial points. Such methods rely heavily on the accuracy of fiducial detection, which is still an open problem due to the difficulty in exact localization of wave boundaries. This paper presents a systematic analysis for human identification from ECG data. A fiducial-detection-based framework that incorporates analytic and appearance attributes is first introduced. The appearance-based approach needs detection of one fiducial point only. Further, to completely relax the detection of fiducial points, a new approach based on autocorrelation (AC) in conjunction with discrete cosine transform (DCT) is proposed. Experimentation demonstrates that the AC/DCT method produces comparable recognition accuracy with the fiducial-detection-based approach.

## 1. INTRODUCTION

Biometric recognition provides airtight security by identifying an individual based on the physiological and/or behavioral characteristics [1]. A number of biometrics modalities have been investigated in the past, examples of which include physiological traits such as face, fingerprint, iris, and behavioral characteristics like gait and keystroke. However, these biometrics modalities either can not provide reliable performance in terms of recognition accuracy (e.g., gait, keystroke) or are not robust enough against falsification. For instance, face is sensitive to artificial disguise, fingerprint can be recreated using latex, and iris can be falsified by using contact lenses with copied iris features printed on.

Analysis of electrocardiogram (ECG) as a tool for clinical diagnosis has been an active research area in the past two decades. Recently, a few proposals [2–7] suggested the possibility of using ECG as a new biometrics modality for human identity recognition. The validity of using ECG for biometric recognition is supported by the fact that the physiological and geometrical differences of the heart in different individuals display certain uniqueness in their ECG signals [8].

Human individuals present different patterns in their ECG regarding wave shape, amplitude, $PT$ interval, due to the difference in the physical conditions of the heart [9]. Also, the permanence characteristic of ECG pulses of a person was studied in [10], by noting that the similarities of healthy subject's pulses at different time intervals, from 0 to 118 days, can be observed when they are plotted on top of each other. These results suggest the distinctiveness and stability of ECG as a biometrics modality. Further, ECG signal is a life indicator, and can be used as a tool for liveness detection. Comparing with other biometric traits, the ECG of a human is more universal, and difficult to be falsified by using fraudulent methods. An ECG-based biometric recognition system can find wide applications in physical access control, medical records management, as well as government and forensic applications.

To build an efficient human identification system, the extraction of features that can truly represent the distinctive characteristics of a person is a challenging problem. Previously proposed methods for ECG-based identity recognition use attributes that are temporal and amplitude distances between detected fiducial points [2–7]. Firstly, focusing on only
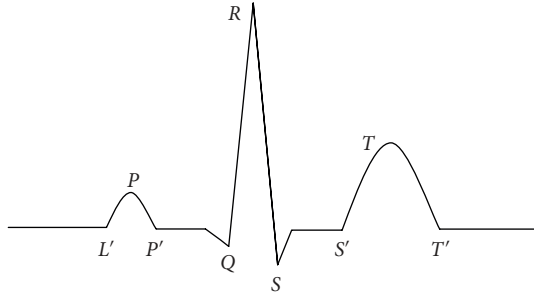
FIGURE 1: Basic shape of an ECG heartbeat signal.

a few fiducial points, the representation of discriminant characteristics of ECG signal might be inadequate. Secondly, their methods rely heavily on the accurate localization of wave boundaries, which is generally very difficult. In this paper, we present a systematic analysis for ECG-based biometric recognition. An analytic-based method that combines temporal and amplitude features is first presented. The analytic features capture local information in a heartbeat signal. As such, the performance of this method depends on the accuracy of fiducial points detection and discriminant power of the features. To address these problems, an appearance-based feature extraction method is suggested. The appearance-based method captures the holistic patterns in a heartbeat signal, and only the detection of the peak is necessary. This is generally easier since $R$ corresponds to the highest and sharpest peak in a heartbeat. To better utilize the complementary characteristics of different types of features and improve the recognition accuracy, we propose a hierarchical scheme for the integration of analytic and appearance attributes. Further, a novel method that does not require any waveform detection is proposed. The proposed approach depends on estimating and comparing the significant coefficients of the discrete cosine transform (DCT) of the autocorrelated heartbeat signals. The feasibility of the introduced solutions is demonstrated using ECG data from two public databases, PTB [11] and MIT-BIH [12]. Experimentation shows that the proposed methods produce promising results.

The remainder of this paper is organized as follows. Section 2 gives a brief description of fundamentals of ECG. Section 3 provides a review of related works. The proposed methods are discussed in Section 4. In Section 5, we present the experimental results along withdetailed discussion. Conclusion and future works are presented in Section 6.

## 2. ECG BASICS

An electrocardiogram (ECG) signal describes the electrical activity of the heart. The electrical activity is related to the impulses that travel through the heart. It provides information about the heart rate, rhythm, and morphology. Normally, ECG is recorded by attaching a set of electrodes on the body surface such as chest, neck, arms, and legs.

A typical ECG wave of a normal heartbeat consists of a $P$ wave, a $QRS$ complex, and a $T$ wave. Figure 1 depicts the basic shape of a healthy ECG heartbeat signal. The $P$

wave reflects the sequential depolarization of the right and left atria. It usually has positive polarity, and its duration is less than 120 milliseconds. The spectral characteristic of a normal $P$ wave is usually considered to be low frequency, below 10–15 Hz. The $QRS$ complex corresponds to depolarization of the right and left ventricles. It lasts for about 70–110 milliseconds in a normal heartbeat, and has the largest amplitude of the ECG waveforms. Due to its steep slopes, the frequency content of the $QRS$ complex is considerably higher than that of the other ECG waves, and is mostly concentrated in the interval of 10–40 Hz. The $T$ wave reflects ventricular repolarization and extends about 300 milliseconds after the $QRS$ complex. The position of the $T$ wave is strongly dependent on heart rate, becoming narrower and closer to the $QRS$ complex at rapid rates [13].

## 3. RELATED WORKS

Although extensive studies have been conducted for ECG based clinical applications, the research for ECG-based biometric recognition is still in its infant stage. In this section, we provide a review of the related works.

Biel et al. [2] are among the earliest effort that demonstrates the possibility of utilizing ECG for human identification purposes. A set of temporal and amplitude features are extracted from a SIEMENS ECG equipment directly. A feature selection algorithm based on simple analysis of correlation matrix is employed to reduce the dimensionality of features. Further selection of feature set is based on experiments. A multivariate analysis-based method is used for classification. The system was tested on a database of 20 persons, and 100% identification rate was achieved by using empirically selected features. A major drawback of Biel et al.'s method is the lack of automatic recognition due to the employment of specific equipment for feature extraction. This limits the scope of applications.

Irvine et al. [3] introduced a system to utilize heart rate variability (HRV) as a biometric for human identification. Israel et al. [4] subsequently proposed a more extensive set of descriptors to characterize ECG trace. An input ECG signal is first preprocessed by a bandpass filter. The peaks are established by finding the local maximum in a region surrounding each of the $P$, $R$, $T$ complexes, and minimum radius curvature is used to find the onset and end of $P$ and $T$ waves. A total number of 15 features, which are time duration between detected fiducial points, are extracted from each heartbeat. A Wilks' Lambda method is applied for feature selection and linear discriminant analysis for classification. This system was tested on a database of 29 subjects with 100% human identification rate and around 81% heartbeat recognition rate can be achieved. In a later work, Israel et al. [5] presented a multimodality system that integrate face and ECG signal for biometric identification. Israel et al.'s method provides automatic recognition, but the identification accuracy with respect to heartbeat is low due to the insufficient representation of the feature extraction methods.

Shen et al. [6] introduced a two-step scheme for identity verification from one-lead ECG. A template matching method is first used to compute the correlation coefficient for

comparison of two *QRS* complexes. A decision-based neural network (DBNN) approach is then applied to complete the verification from the possible candidates selected with template matching. The inputs to the DBNN are seven temporal and amplitude features extracted from *QRST* wave. The experimental results from 20 subjects showed that the correct verification rate was 95% for template matching, 80% for the DBNN, and 100% for combining the two methods. Shen [7] extended the proposed methods in a larger database that contains 168 normal healthy subjects. Template matching and mean square error (MSE) methods were compared for prescreening, and distance classification and DBNN compared for second-level classification. The features employed for the second-level classification are seventeen temporal and amplitude features. The best identification rate for 168 subjects is 95.3% using template matching and distance classification.

In summary, existing works utilize feature vectors that are measured from different parts of the ECG signal for classification. These features are either time duration, or amplitude differences between fiducial points. However, accurate fiducial detection is a difficult task since current fiducial detection machines are built solely for the medical field, where only the approximate locations of fiducial points are required for diagnostic purposes. Even if these detectors are accurate in identifying exact fiducial locations validated by cardiologists, there is no universally acknowledged rule for defining exactly where the wave boundaries lie [14]. In this paper, we first generalize existing works by applying similar analytic features, that is, temporal and amplitude distance attributes. Our experimentation shows that by using analytic features alone, reliable performance cannot be obtained. To improve the identification accuracy, an appearance-based approach which only requires detection of the *R* peak is introduced, and a hierarchical classification scheme is proposed to integrate the two streams of features. Finally, we present a method that does not need any fiducial detection. This method is based on classification of coefficients from the discrete cosine transform (DCT) of the autocorrelation (AC) sequence of windowed ECG data segments. As such, it is insensitive to heart rate variations, simple and computationally efficient. Computer simulations demonstrate that it is possible to achieve high recognition accuracy without pulse synchronization.

## 4. METHODOLOGY

Biometrics-based human identification is essentially a pattern recognition problem which involves preprocessing, feature extraction, and classification. Figure 2 depicts the general block diagram of the proposed methods. In this paper, we introduce two frameworks, namely, feature extraction with/without fiducial detection, for ECG-based biometric recognition.

### 4.1. Preprocessing

The collected ECG data usually contain noise, which include low-frequency components that cause baseline wander, and high-frequency components such as power-line interfer-



FIGURE 2: Block diagram of proposed systems.

ences. Generally, the presence of noise will corrupt the signal, and make the feature extraction and classification less accurate. To minimize the negative effects of the noise, a denoising procedure is important. In this paper, we use a Butterworth bandpass filter to perform noise reduction. The cutoff frequencies of the bandpass filter are selected as 1 Hz–40 Hz based on empirical results. The first and last heartbeats of the denoised ECG records are eliminated to get full heartbeat signals. A thresholding method is then applied to remove the outliers that are not appropriate for training and classification. Figure 3 gives a graphical illustration of the applied preprocessing approach.

### 4.2. Feature extraction based on fiducial detection

After preprocessing, the *R* peaks of an ECG trace are localized by using a *QRS* detector, ECGPUWAVE [15, 16]. The heartbeats of an ECG record are aligned by the *R* peak position and truncated by a window of 800 milliseconds centered at *R*. This window size is estimated by heuristic and empirical results such that the *P* and *T* waves can also be included and therefore most of the information embedded in heartbeats is retained [17].

#### 4.2.1. Analytic feature extraction

For the purpose of comparative study, we follow similar feature extraction procedure as described in [4, 5]. The fiducial points are depicted in Figure 1. As we have detected the *R* peak, the *Q*, *S*, *P*, and *T* positions are localized by finding local maxima and minima separately. To find the $L'$, $P'$, $S'$, and $T'$ points, we use a method as shown in Figure 4(a). The *X* and *Z* points are fixed and we search downhill from *X* to find the point that maximizes the sum of distances $a + b$. Figure 4(b) gives an example of fiducial points localization.

The extracted attributes are temporal and amplitude distances between these fiducial points. The 15 temporal features are exactly the same as described in [4, 5], and they are normalized by $P'T'$ distance to provide less variability with respect to heart rate. Figure 5 depicts these attributes graphically, while Table 1 lists all the extracted analytic features.

#### 4.2.2. Appearance feature extraction

Principal component analysis (PCA) and linear discriminant analysis (LDA) are transform domain methods for data reduction and feature extraction. PCA is an unsupervised learning technique which provides an optimal, in the least mean square error sense, representation of the input in a lower-dimensional space. Given a training set $\mathcal{Z} = \{\mathcal{Z}_i\}_{i=1}^{C}$, containing *C* classes with each class $\mathcal{Z}_i = \{\mathbf{z}_{ij}\}_{j=1}^{C_i}$ consisting of a number of heartbeats $\mathbf{z}_{ij}$, a total of $N = \sum_{i=1}^{C} C_i$

TABLE 1: List of extracted analytic features.

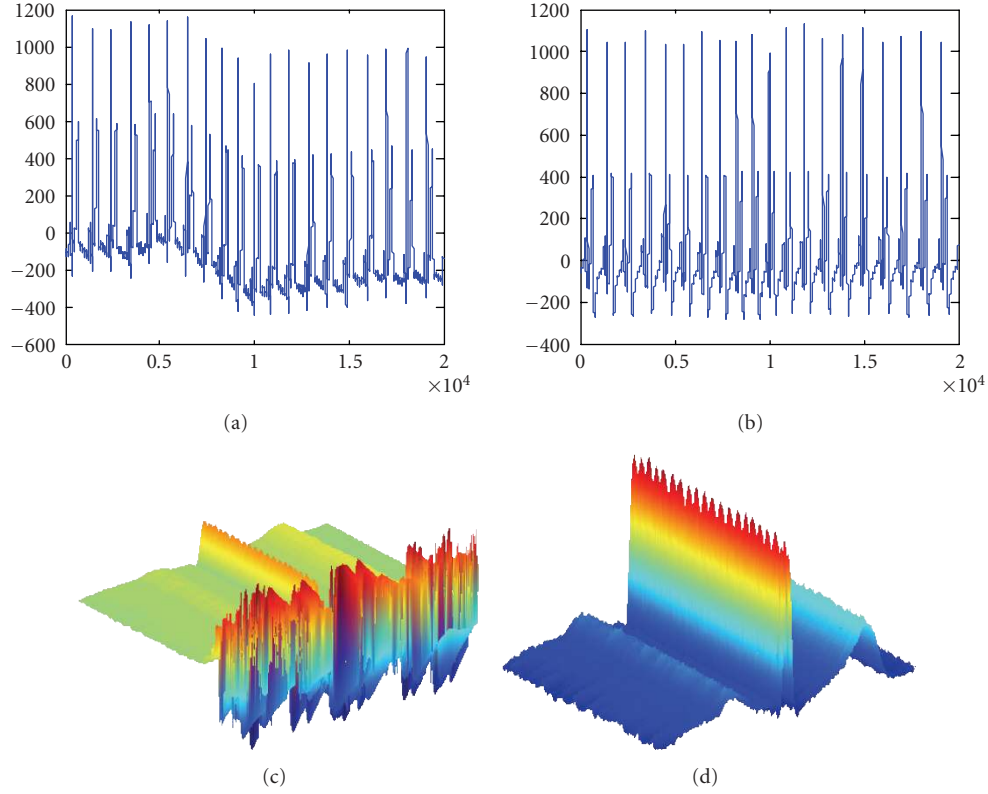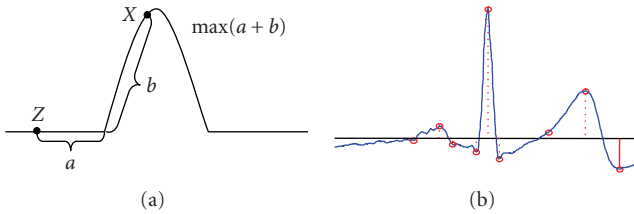| | Extracted features | | | |
|---|---|---|---|---|
| Temporal | 1. $RQ$ | 4 $RL'$ | 7. $RS'$ | 10. $S'T'$ | 13. $PT$ |
| | 2. $RS$ | 5. $RP'$ | 8. $RT'$ | 11. $ST$ | 14. $LQ$ |
| | 3. $RP$ | 6. $RT$ | 9. $L'P'$ | 12. $PQ$ | 15. $ST'$ |
| Amplitude | 16. $PL'$ | | 17. $PQ$ | | 18. $RQ$ |
| | 19. $RS$ | | 20. $TS$ | | 21. $TT'$ |



(a)



(b)



(c)



(d)

FIGURE 3: Preprocessing ((a) original signal; (b) noise reduced signal; (c) original $R$-peak aligned signal; (d) $R$-peak aligned signal after outlier removal).



(a)



(b)

FIGURE 4: Fiducial points determination.

heartbeats, the PCA is applied to the training set $\mathbb{Z}$ to find the $M$ eigenvectors of the covariance matrix

$$\mathbf{S}_{\text{cov}} = \frac{1}{N} \sum_{i=1}^{C} \sum_{j=1}^{C_i} (\mathbf{z}_{ij} - \bar{\mathbf{z}})(\mathbf{z}_{ij} - \bar{\mathbf{z}})^T, \quad (1)$$

where $\bar{\mathbf{z}} = 1/N \sum_{i=1}^{C} \sum_{j=1}^{C_i} \mathbf{z}_{ij}$ is the average of the ensemble. The eigen heartbeats are the first $M(\leq N)$ eigenvectors corre-

sponding to the largest eigenvalues, denoted as $\Psi$. The original heartbeat is transformed to the $M$-dimension subspace by a linear mapping

$$\mathbf{y}_{ij} = \Psi^T (\mathbf{z}_{ij} - \bar{\mathbf{z}}), \quad (2)$$

where the basis vectors $\Psi$ are orthonormal. The subsequent classification of heartbeat patterns can be performed in the transformed space [18].

LDA is another representative approach for dimension reduction and feature extraction. In contrast to PCA, LDA utilizes supervised learning to find a set of $M$ feature basis vectors $\{\psi_m\}_{m=1}^{M}$ in such a way that the ratio of between-class and within-class scatters of the training sample set is maximized. The maximization is equivalent to solve the following eigenvalue problem

$$\Psi = \arg\max_{\psi} \frac{|\Psi^T \mathbf{S}_b \Psi|}{|\Psi^T \mathbf{S}_w \Psi|}, \quad \Psi = \{\psi_1, \dots, \psi_M\}, \quad (3)$$
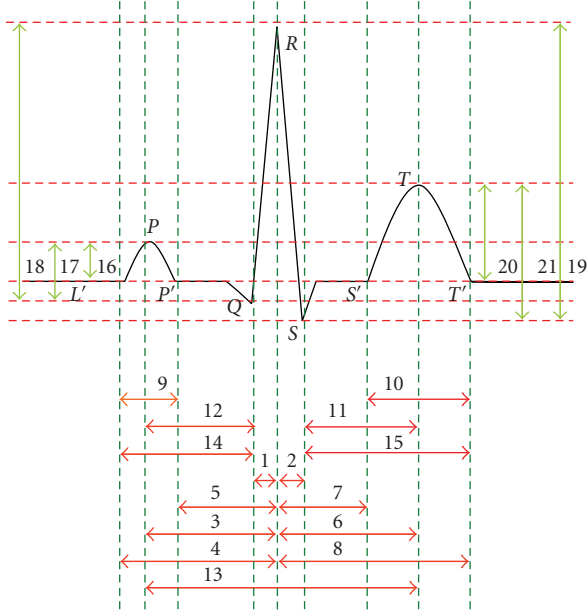
FIGURE 5: Graphical demonstration of analytic features.

where $\mathbf{S}_b$ and $\mathbf{S}_w$ are between-class and within-class scatter matrices, and can be computed as follows:

$$
\begin{aligned}
\mathbf{S}_b &= \frac{1}{N} \sum_{i=1}^{C} C_i (\bar{\mathbf{z}}_i - \bar{\mathbf{z}}) (\bar{\mathbf{z}}_i - \bar{\mathbf{z}})^T, \\
\mathbf{S}_w &= \frac{1}{N} \sum_{i=1}^{C} \sum_{j=1}^{C_i} (\mathbf{z}_{ij} - \bar{\mathbf{z}}_i) (\mathbf{z}_{ij} - \bar{\mathbf{z}}_i)^T,
\end{aligned}
\tag{4}
$$

where $\bar{\mathbf{z}}_i = 1/C_i \sum_{j=1}^{C_i} \mathbf{z}_{ij}$ is the mean of class $\mathcal{Z}_i$. When $\mathbf{S}_w$ is nonsingular, the basis vectors $\Psi$ sought in (3) correspond to the first $M$ most significant eigenvectors of $(\mathbf{S}_w^{-1} \mathbf{S}_b)$, where the "significant" means that the eigenvalues corresponding to these eigenvectors are the first $M$ lagest ones. For an input heartbeat $\mathbf{z}$, its LDA-based feature representation can be obtained simply by a linear projection, $\mathbf{y} = \Psi^T \mathbf{z}$ [18].

### 4.3. Feature extraction without fiducial detection

The proposed method for feature extraction without fiducial detection is based on a combination of autocorrelation and discrete cosine transform. We refer to this method as the AC/DCT method [19]. The AC/DCT method involves four stages: (1) windowing, where the preprocessed ECG trace is segmented into nonoverlapping windows, with the only restriction that the window has to be longer than the average heartbeat length so that multiple pulses are included; (2) estimation of the normalized autocorrelation of each window; (3) discrete cosine transform over $\mathcal{L}$ lags of the autocorrelated signal; and (4) classification based on significant coefficients of DCT. A graphical demonstration of different stages is presented in Figure 6.

The ECG is a nonperiodic but highly repetitive signal. The motivation behind the employment of autocorrelation-based features is to detect the nonrandom patterns. Autocorrelation embeds information about the most representative characteristics of the signal. In addition, AC is used to blend into a sequence of sums of products samples that would otherwise need to be subjected to fiducial detection. In other words, it provides an automatic shift invariant accumulation of similarity features over multiple heartbeat cycles. The autocorrelation coefficients $\hat{R}_{xx}[m]$ can be computed as follows:

$$
\hat{R}_{xx}[m] = \frac{\sum_{i=0}^{N-|m|-1} x[i] x[i+m]}{\hat{R}_{xx}[0]},
\tag{5}
$$

where $x[i]$ is the windowed ECG for $i = 0, 1, \ldots, (N - |m| - 1)$, $x[i+m]$ is the time-shifted version of the windowed ECG with a time lag of $m = 0, 1, \ldots, \mathcal{L} - 1)$, $\mathcal{L} \ll N$. The division with the maximum value, $\hat{R}_{xx}[0]$, cancels out the biasing factor and this way either *biased* or *unbiased* autocorrelation estimation can be performed. The main contributors to the autocorrelated signal are the $P$ wave, the $QRS$ complex, and the $T$ wave. However, even among the pulses of the same subject, large variations in amplitude present and this makes normalization a necessity. It should be noted that a window is allowed to blindly cut out the ECG record, even in the middle of a pulse. This alone releases the need for exact heartbeat localization.

Our expectations for the autocorrelation, to embed similarity features among records of the same subject, are confirmed by the results of Figure 7, which shows the $\hat{R}_{xx}[m]$ obtained from different ECG windows of the same subject from two different records in the PTB database taken at a different time.

Autocorrelation offers information that is very important in distinguishing subjects. However, the dimensionality of autocorrelation features is considerably high (e.g., $\mathcal{L} = 100, 200, 300$). The discrete cosine transform is then applied to the autocorrelation coefficients for dimensionality reduction. The frequency coefficients are estimated as follows:

$$
Y[u] = G[u] \sum_{i=0}^{N-1} y[i] \frac{\pi \cos(2i+1)u}{2N},
\tag{6}
$$

where $N$ is the length of the signal $y[i]$ for $i = 0, 1, \ldots, (N - |m| - 1)$. For the AC/DCT method $y[i]$ is the autocorrelated ECG obtained from (5). $G[u]$ is given from

$$
G(k) = \begin{cases} \sqrt{\dfrac{1}{N}}, & k = 0, \\ \sqrt{\dfrac{2}{N}}, & 1 \le k \le N - 1. \end{cases}
\tag{7}
$$

The energy compaction property of DCT allows representation in lower dimensions. This way, near zero components of the frequency representation can be discarded and the number of important coefficients is eventually reduced. Assuming we take an $\mathcal{L}$-point DCT of the autocorrelated signal, only $\mathcal{K} \ll \mathcal{L}$ nonzero DCT coefficients will contain significant information for identification. Ideally, from a frequency domain perspective, the $\mathcal{K}$ most significant coefficients will correspond to the frequencies between the bounds of the bandpass filter that was used in preprocessing. This is

(a) 5 seconds of ECG from subject A



(b) 5 seconds of ECG from subject B



(c) AC of A



(d) AC of B



(e) 300 AC Coefficients of A



(f) 300 AC Coefficients of B


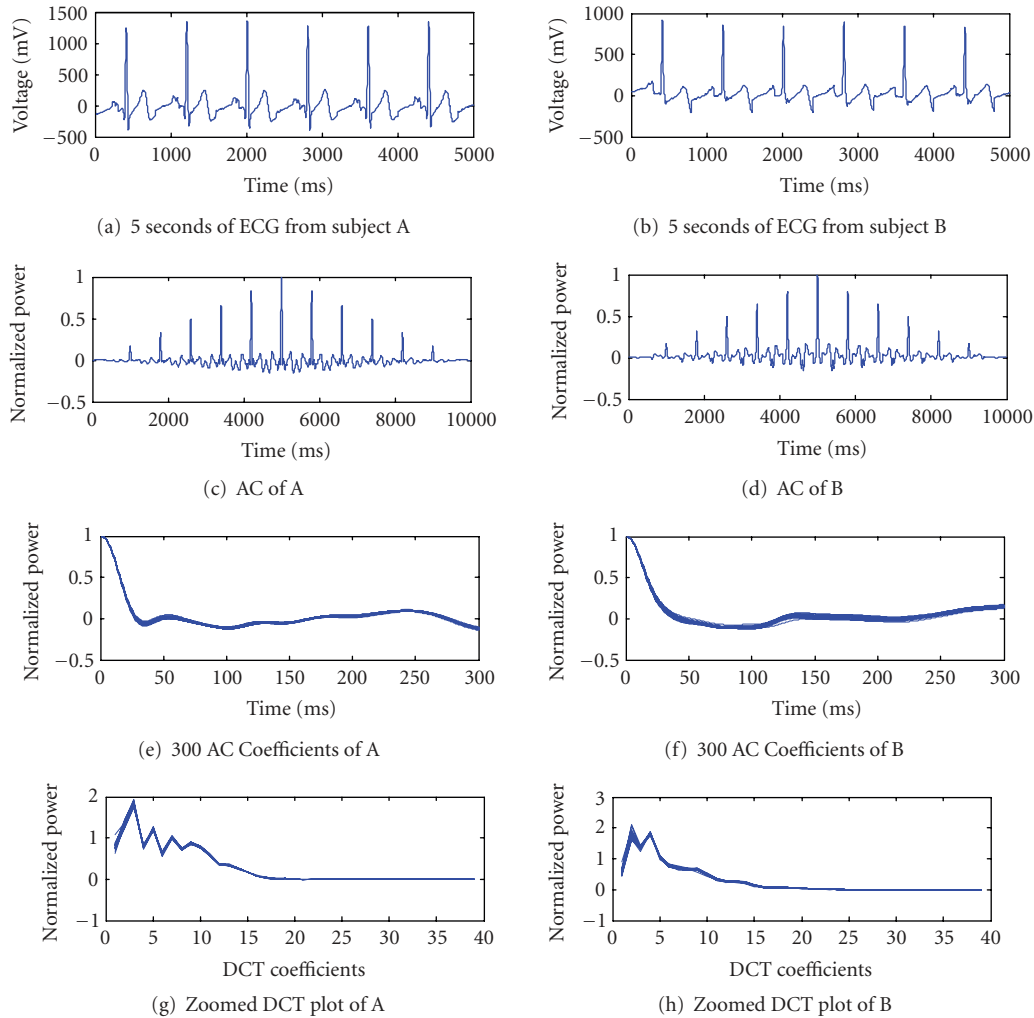
(g) Zoomed DCT plot of A



(h) Zoomed DCT plot of B

FIGURE 6: (a-b) 5 seconds window of ECG from two subjects of the PTB dataset, subject A and B. (c-d) The normalized autocorrelation sequence of A and B. (e-f) Zoom in to 300 AC coefficients from the maximum form different windows of subject A and B. (g-h) DCT of the 300 AC coefficients from all ECG windows of subject A and B, including the windows on top. Notice that the same subject has similar AC and DCT shape.

because after the AC operation, the bandwidth of the signal remained the same.

## 5.  EXPERIMENTAL RESULTS

To evaluate the performance of the proposed methods, we conducted our experiments on two sets of public databases: PTB [11] and MIT-BIH [12]. The PTB database is offered from the National Metrology Institute of Germany and it contains 549 records from 294 subjects. Each record of the PTB database consists of the conventional 12-leads and 3 Frank leads ECG. The signals were sampled at 1000 Hz with a resolution of $0.5 \mu$V. The duration of the recordings vary for each subject. The PTB database contains a large collection of healthy and diseased ECG signals that were collected at the Department of Cardiology of University Clinic Benjamin Franklin in Berlin. A subset of 13 healthy subjects of different age and sex was selected from the database to test our methods. The criteria for data selec-

tion are healthy ECG waveforms and at least two recordings for each subject. In our experiments, we use one record from each subject to form the gallery set, and another record for the testing set. The two records were collected a few years apart.

The MIT-BIH Normal Sinus Rhythm Database contains 18 ECG recordings from different subjects. The recordings of the MIT database were collected at the Arrhythmia Laboratory of Boston's Beth Israel Hospital. The subjects included in the database did not exhibit significant arrhythmias. The MIT- BIH Normal Sinus Rhythm Database was sampled at 128 Hz. A subset of 13 subjects was selected to test our methods. The selection of data was based on the length of the recordings. The waveforms of the remaining recordings have many artifacts that reduce the valid heartbeat information, and therefore were not used in our experiments. Since the database only offers one record for each subject, we partitioned each record into two halves and use the first half as the gallery set and the second half as the testing set.
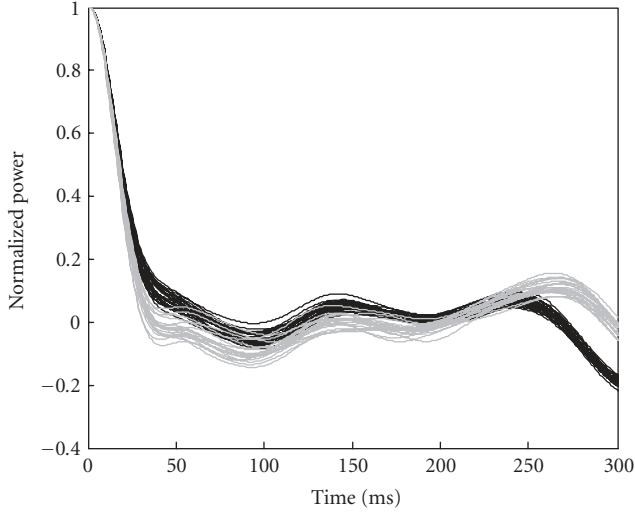
FIGURE 7: AC sequences of two different records taken at different times from the same subject of the PTB dataset. Sequences from the same record are plotted in the same shade.

## 5.1. Feature extraction based on fiducial detection

In this section, we present experimental results by using features extracted with fiducial points detection. The evaluation is based on subject and heartbeat recognition rate. Subject recognition accuracy is determined by majority voting, while heartbeat recognition rate corresponds to the percentage of correctly identified individual heartbeat signals.

### 5.1.1. Analytic features

To provide direct comparison with existing works [4, 5], experiments were first performed on the 15 temporal features only, using a Wilks' Lambda-based stepwise method for feature selection, and linear discriminant analysis (LDA) for classification. Wilks' Lambda measures the differences between the mean of different classes on combinations of dependent variables, and thus can be used as a test of the significance of the features. In Section 4.2.2, we have discussed the LDA method for feature extraction. When LDA is used as a classifier, it assumes a discriminant function for each class as a linear function of the data. The coefficients of these functions can be found by solving the eigenvalue problem as in (3). An input data is classified into the class that gives the greatest discriminant function value. When LDA is used for classification, it is applied on the extracted features, while for feature extraction, it is applied on the original signal.

In this paper, the Wilks' Lambda-based feature selection and LDA-based classification are implemented in SPSS (a trademark of SPSS Inc. USA). In our experiments, the 15 temporal features produce subject recognition rate of 84.61% and 100%, and heartbeat recognition rate of 74.45% and 74.95% for PTB and MIT-BIH datasets, respectively.

Figure 8 shows the contingency matrices when only temporal features are used. It can be observed that the heartbeats of an individual are confused with many other subjects. Only

the heartbeats from 2 subjects in PTB and 1 subject in MIT-BIH are 100% correctly identified. This demonstrates that the extracted temporal features cannot efficiently distinguish different subjects. In our second experiment, we add amplitude attributes to the feature set. This approach achieves significant improvement with subject recognition rate of 100% for both datasets, heartbeat recognition rate of 92.40% for PTB, and 94.88% for MIT-BIH. Figure 9 shows the all-class scatter plot in the two experiments. It is clear that different classes are much better separated by including amplitude features.

### 5.1.2. Appearance features

In this paper, we compare the performance of PCA and LDA using the nearest neighbor (NN) classifier. The similarity measure is based on Euclidean distance. An important issue in appearance-based approaches is how to find the optimal parameters for classification. For a $C$ class problem, LDA can reduce the dimensionality to $C - 1$ due to the fact that the rank of the between-class matrix cannot go beyond $C - 1$. However, these $C - 1$ parameters might not be the optimal ones for classification. Exhaustive search is usually applied to find the optimal LDA-domain features. In PCA parameter determination, we use a criterion by taking the first $M$ eigenvectors that satisfy $\sum_{i=1}^{M} \lambda_i / \sum_{i=1}^{N} \lambda_i \geq 99\%$, where $\lambda_i$ is the eigenvalue and $N$ is the dimensionality of feature space.

Table 2 shows the experimental results of applying PCA and LDA on PTB and MIT-BIH datasets. Both PCA and LDA achieve better identification accuracy than analytic features. This reveals that the appearance-based analysis is a good tool for human identification from ECG. Although LDA is class specific and normally performs better than PCA in face recognition problems [18], since PCA performs better in our particular problem, we use PCA for the analysis hereafter.

### 5.1.3. Feature integration

Analytic and appearance-based features are two complementary representations of the characteristics of the ECG data. Analytic features capture local information, while appearance features represent holistic patterns. An efficient integration of these two streams of features will enhance the recognition performance. A simple integration scheme is to concatenate the two streams of extracted features into one vector and perform classification. The extracted analytic features include both temporal and amplitude attributes. For this reason, it is not suitable to use a distance metric for classification since some features will overpower the results. We therefore use LDA as the classifier, and Wilks' Lambda for feature selection. This method achieves heartbeat recognition rate of 96.78% for PTB and 97.15% for MIT-BIH. The subject recognition rate is 100% for both datasets. In the MIT-BIH dataset, the simple concatenation method actually degrades the performance than PCA only. This is due to the suboptimal characteristic of the feature selection method, by which optimal feature set cannot be obtained.

To better utilize the complementary characteristics of analytic and appearance attributes, we propose a hierarchical

TABLE 2: Experimental results of PCA and LDA.

| | PTB | | MIT-BIH | |
|---|---|---|---|---|
| | Subject | Heartbeat | Subject | Heartbeat |
| PCA | 100% | 95.55% | 100% | 98.48% |
| LDA | 100% | 93.01% | 100% | 98.48% |

Known inputs

| | 1 | 2 | 3 | 4 | 5 | 6 | 7 | 8 | 9 | 10 | 11 | 12 | 13 |
|---|---|---|---|---|---|---|---|---|---|---|---|---|---|
| 1 | 96 | 0 | 0 | 0 | 2 | 0 | 0 | 0 | 3 | 0 | 41 | 0 | 1 |
| 2 | 0 | 84 | 1 | 0 | 19 | 3 | 0 | 4 | 2 | 17 | 0 | 0 | 0 |
| 3 | 0 | 20 | 100 | 0 | 2 | 2 | 0 | 0 | 9 | 0 | 0 | 0 | 0 |
| 4 | 1 | 4 | 0 | 94 | 3 | 0 | 0 | 0 | 2 | 21 | 15 | 0 | 2 |
| 5 | 0 | 0 | 0 | 0 | 23 | 0 | 0 | 0 | 0 | 1 | 0 | 0 | 0 |
| 6 | 0 | 0 | 5 | 5 | 1 | 107 | 0 | 1 | 0 | 0 | 0 | 0 | 0 |
| 7 | 0 | 0 | 0 | 6 | 41 | 5 | 114 | 0 | 0 | 4 | 0 | 0 | 8 |
| 8 | 0 | 0 | 1 | 18 | 2 | 0 | 0 | 110 | 4 | 3 | 0 | 0 | 0 |
| 9 | 1 | 1 | 0 | 0 | 0 | 0 | 0 | 0 | 21 | 0 | 15 | 0 | 0 |
| 10 | 0 | 0 | 0 | 0 | 2 | 0 | 0 | 0 | 0 | 61 | 0 | 0 | 4 |
| 11 | 21 | 0 | 0 | 0 | 0 | 0 | 0 | 0 | 22 | 0 | 79 | 0 | 0 |
| 12 | 0 | 0 | 0 | 0 | 0 | 1 | 0 | 0 | 0 | 0 | 0 | 91 | 0 |
| 13 | 10 | 0 | 0 | 0 | 2 | 0 | 0 | 0 | 0 | 13 | 2 | 0 | 107 |

Detected output

PTB: subject recognition rate: 11/13 = 84.61%, heartbeat recognition rate: 74.45%

(a)

Known inputs

| | 1 | 2 | 3 | 4 | 5 | 6 | 7 | 8 | 9 | 10 | 11 | 12 | 13 |
|---|---|---|---|---|---|---|---|---|---|---|---|---|---|
| 1 | 30 | 0 | 5 | 0 | 0 | 0 | 0 | 0 | 0 | 0 | 0 | 0 | 0 |
| 2 | 0 | 23 | 0 | 0 | 0 | 0 | 0 | 0 | 2 | 0 | 2 | 0 | 0 |
| 3 | 14 | 20 | 35 | 0 | 2 | 2 | 0 | 0 | 9 | 0 | 0 | 1 | 1 |
| 4 | 0 | 0 | 0 | 33 | 0 | 1 | 0 | 0 | 2 | 0 | 3 | 0 | 1 |
| 5 | 0 | 0 | 0 | 0 | 28 | 0 | 1 | 1 | 0 | 0 | 0 | 0 | 5 |
| 6 | 0 | 0 | 0 | 0 | 1 | 38 | 1 | 0 | 0 | 0 | 0 | 0 | 1 |
| 7 | 1 | 0 | 2 | 3 | 4 | 0 | 22 | 0 | 0 | 0 | 0 | 5 | 9 |
| 8 | 1 | 0 | 1 | 0 | 0 | 0 | 0 | 30 | 0 | 0 | 0 | 0 | 0 |
| 9 | 0 | 4 | 0 | 3 | 0 | 0 | 0 | 0 | 26 | 0 | 1 | 0 | 2 |
| 10 | 0 | 0 | 0 | 1 | 0 | 0 | 0 | 0 | 1 | 35 | 0 | 0 | 1 |
| 11 | 0 | 3 | 0 | 7 | 0 | 0 | 0 | 0 | 1 | 0 | 35 | 2 | 0 |
| 12 | 0 | 0 | 0 | 0 | 2 | 0 | 1 | 1 | 0 | 0 | 0 | 38 | 0 |
| 13 | 1 | 0 | 1 | 0 | 13 | 0 | 12 | 1 | 0 | 0 | 0 | 6 | 22 |

Detected output

MIT-BIH: subject recognition rate: 13/13 = 100%, heartbeat recognition rate: 74.95%

(b)

FIGURE 8: Contingency matrices by using temporal features only.

scheme for feature integration. A central consideration in our development of classification scheme is trying to change a large-class-number problem into a small-class-number problem. In pattern recognition, when the number of classes is large, the boundaries between different classes tend to be complex and hard to separate. It will be easier if we can reduce the possible number of classes and perform classification in a smaller scope [17]. Using a hierarchical architecture, we can first classify the input into a few potential classes, and a second-level classification can be performed within these candidates.

Figure 10 shows the diagram of the proposed hierarchical scheme. At the first step, only analytic features are used for classification. The output of this first-level classification provides the candidate classes that the entry might belong to. If all the heartbeats are classified as one subject, the decision module outputs this result directly. If the heartbeats are classified as a few different subjects, a new PCA-based classification module, which is dedicated to classify these confused subjects, is then applied. We select to perform classification using analytic features first due to the simplicity in feature selection. A feature selection in each of the possible combinations of the classes is computationally complex. By using PCA, we can easily set the parameter selection as one criterion and important information can be retained. This is well supported by our experimental results. The proposed hierarchical scheme achieves subject recognition rate of 100% for both datasets, and heartbeat recognition accuracy of 98.90% for PTB and 99.43% for MIT-BIH.

A diagrammatic comparison of various feature sets and classification schemes is shown in Figure 11. The proposed hierarchical scheme produces promising results in heartbeat recognition. This "divide and conquer" mechanism maps global classification into local classification and thus reduces the complexity and difficulty. Such hierarchical architecture is general and can be applied to other pattern recognition problems as well.

### 5.2. *Feature extraction without fiducial detection*

In this section, the performance of the AC/DCT method is reported. The similarity measure is based on normalized
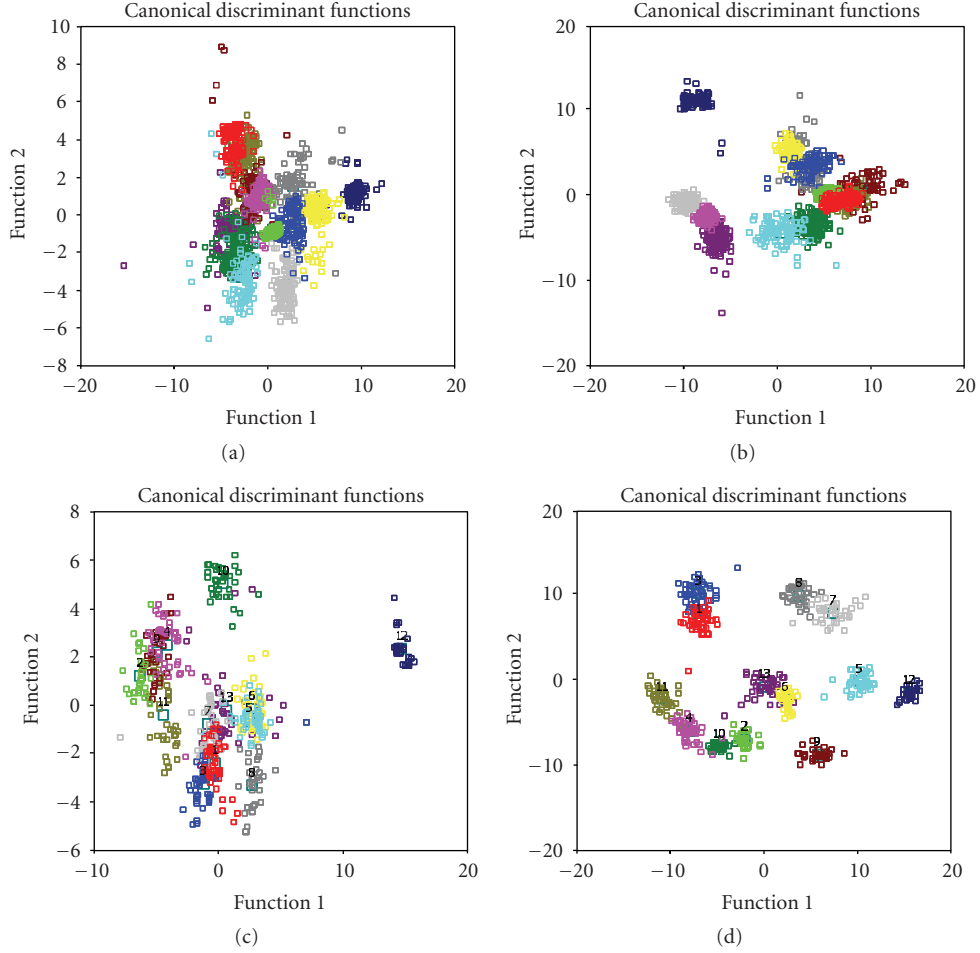
FIGURE 9: All-class scatter plot ((a)-(b) PTB; (c)-(d) MIT-BIH; (a)-(c) temporal features only; (b)-(d) all analytic features).

TABLE 3: Experimental results from classification of the PTB dataset using different AC lags.

| $\mathcal{L}$ | $\mathcal{K}$ | Subject recognition rate | Window recognition rate |
|---|---|---|---|
| 60 | 5 | 11/13 | 176/217 |
| 90 | 8 | 11/13 | 173/217 |
| 120 | 10 | 11/13 | 175/217 |
| 150 | 12 | 12/13 | 189/217 |
| 180 | 15 | 12/13 | 181/217 |
| 210 | 17 | 12/13 | 186/217 |
| **240** | **20** | **13/13** | **205/217** |
| 270 | 22 | 11/13 | 174/217 |
| 300 | 24 | 12/13 | 195/217 |

Euclidean distance, and the nearest neighbor (NN) is used as the classifier. The normalized Euclidean distance between two feature vectors $\mathbf{x}_1$ and $\mathbf{x}_2$ is defined as

$$D(\mathbf{x}_1, \mathbf{x}_2) = \frac{1}{V}\sqrt{(\mathbf{x}_1 - \mathbf{x}_2)^T(\mathbf{x}_1 - \mathbf{x}_2)}, \qquad (8)$$

where $V$ is the dimensionality of the feature vectors, which is the number of DCT coefficients in the proposed method.

This factor is there to assure fair comparisons for different dimensions that $\mathbf{x}$ might have.

By applying a window of 5 milliseconds length with no overlapping, different number of windows are extracted from every subject in the databases. The test sets for classification were formed by a total of 217 and 91 windows from the PTB and MIT-BIH datasets, respectively. Several different window lengths that have been tested show approximately the same

TABLE 4: Experimental results from classification of the MIT-BIH dataset using different AC lags.

| $\mathcal{L}$ | $\mathcal{K}$ | Subject recognition rate | Window recognition rate |
|---|---|---|---|
| **60** | **38** | **13/13** | **89/91** |
| 90 | 57 | 12/13 | 69/91 |
| 120 | 75 | 11/13 | 64/91 |
| 150 | 94 | 13/13 | 66/91 |
| 180 | 113 | 12/13 | 61/91 |
| 210 | 132 | 11/13 | 56/91 |
| 240 | 150 | 8/13 | 44/91 |
| 270 | 169 | 8/13 | 43/91 |
| 300 | 188 | 8/13 | 43/91 |
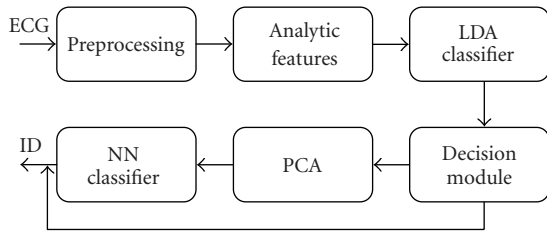


FIGURE 10: Block diagram of hierarchical scheme.
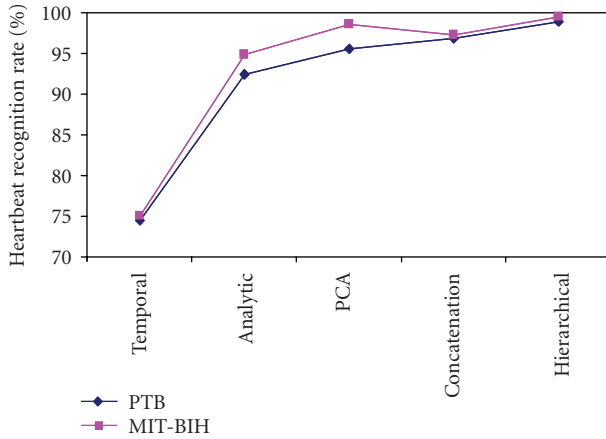


FIGURE 11: Comparison of experimental results.



FIGURE 12: 3D plot of DCT coefficients from 13 subjects of the PTB dataset.

classification performance, as long as multiple pulses are included. The normalized autocorrelation has been estimated using (5), over different AC lags. The DCT feature vector of the autocorrelated ECG signal is evaluated and compared to the corresponding DCT feature vectors of all subjects in the database to determine the best match. Figure 12 shows three DCT coefficients for all subjects in the PTB dataset. It can be observed that different classes are well distinguished.

Tables 3 and 4 present the results of the PTB and MIT-BIH datasets, respectively, with $\mathcal{L}$ denotes the time lag for AC computation, and $\mathcal{K}$ represents number of DCT coefficients for classification. The number of DCT coefficients is selected to correspond to the upper bound of the applied bandpas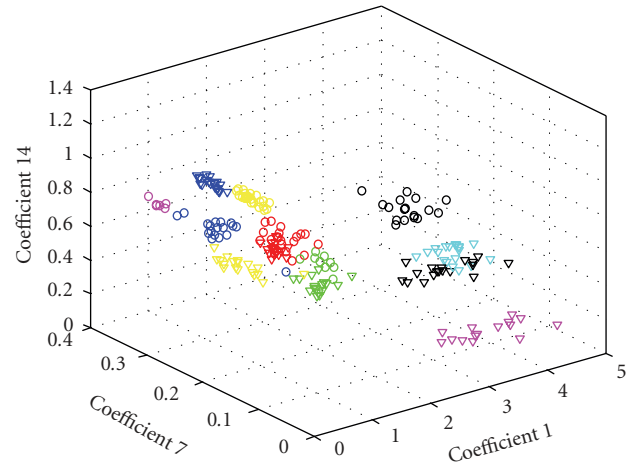s filter, that is, 40 Hz. The highest performance is achieved when an autocorrelation lag of 240 for the PTB and 60 for the MIT-BIH datasets are used. These windows correspond approximately to the *QRS* and *T* wave of each datasets. The difference in the lags that offer highest classification rate between the two datasets is due to the different sampling frequencies.

The results presented in Tables 3 and 4 show that it is possible to have perfect subject identification and very high window recognition rate. The AC/DCT method offers 94.47% and 97.8% window recognition rate for the PTB and MIT-BIH datasets, respectively.

The results of our experiments demonstrate that an ECG-based identification method without fiducial detection is possible. The proposed method provides an efficient, robust and computationally efficient technique for human identification.

## 6. CONCLUSION

In this paper, a systematic analysis of ECG-based biometric recognition was presented. An analytic-based feature extraction approach which involves a combination of temporal and amplitude features was first introduced. This method uses

local information for classification, therefore is very sensitive to the accuracy of fiducial detection. An appearance-based method, which involves the detection of only one fiducial point, was subsequently proposed to capture holistic patterns of the ECG heartbeat signal. To better utilize the complementary characteristics of analytic and appearance attributes, a hierarchical data integration scheme was proposed. Experimentation shows that the proposed methods outperform existing works.

To completely relax fiducial detection, a novel method, termed AC/DCT, was proposed. The AC/DCT method captures the repetitive but nonperiodic characteristic of ECG signal by computing the autocorrelation coefficients. Discrete cosine transform is performed on the autocorrelated signal to reduce the dimensionality while preserving the significant information. The AC/DCT method is performed on windowed ECG segments, and therefore does not need pulse synchronization. Experimental results show that it is possible to perform ECG biometric recognition without fiducial detection. The proposed AC/DCT method offers significant computational advantages, and is general enough to apply to other types of signals, such as acoustic signals, since it does not depend on ECG specific characteristics.

In this paper, the effectiveness of the proposed methods was tested on normal healthy subjects. Nonfunctional factors such as stress and exercise may have impact on the expression of ECG trace. However, other than the changes in the rhythm, the morphology of the ECG is generally unaltered [20]. In the proposed fiducial detection-based method, the temporal features were normalized and demonstrated to be invariant to stress in [4]. For the AC/DCT method, a window selection from the autocorrelation that corresponds to the QRS complex is suggested. Since the QRS complex is less variant to stress, the recognition accuracy will not be effected. In the future, the impact of functional factors, such as aging, cardiac functions, will be studied. Further efforts will be devoted to development and extension of the proposed frameworks with versatile ECG morphologies in nonhealthy human subjects.

## ACKNOWLEDGMENTS

## REFERENCES

[1] A. K. Jain, A. Ross, and S. Prabhakar, "An introduction to biometric recognition," *IEEE Transactions on Circuits and Systems for Video Technology*, vol. 14, no. 1, pp. 4–20, 2004.

[2] L. Biel, O. Pettersson, L. Philipson, and P. Wide, "ECG analysis: a new approach in human identification," *IEEE Transactions on Instrumentation and Measurement*, vol. 50, no. 3, pp. 808–812, 2001.

[3] J. M. Irvine, B. K. Wiederhold, L. W. Gavshon, et al., "Heart rate variability: a new biometric for human identification," in *Proceedings of the International Conference on Artificial Intelligence (IC-AI '01)*, pp. 1106–1111, Las Vegas, Nev, USA, June 2001.

[4] S. A. Israel, J. M. Irvine, A. Cheng, M. D. Wiederhold, and B. K. Wiederhold, "ECG to identify individuals," *Pattern Recognition*, vol. 38, no. 1, pp. 133–142, 2005.

[5] S. A. Israel, W. T. Scruggs, W. J. Worek, and J. M. Irvine, "Fusing face and ECG for personal identification," in *Proceedings of the 32nd Applied Imagery Pattern Recognition Workshop (AIPR '03)*, pp. 226–231, Washington, DC, USA, October 2003.

[6] T. W. Shen, W. J. Tompkins, and Y. H. Hu, "One-lead ECG for identity verification," in *Proceedings of the 2nd Joint Engineering in Medicine and Biology, 24th Annual Conference and the Annual Fall Meeting of the Biomedical Engineering Society (EMBS/BMES '02)*, vol. 1, pp. 62–63, Houston, Tex, USA, October 2002.

[7] T. W. Shen, "Biometric identity verification based on electrocardiogram (ECG)," Ph.D. dissertation, University of Wisconsin, Madison, Wis, USA, 2005.

[8] R. Hoekema, G. J. H. Uijen, and A. van Oosterom, "Geometrical aspects of the interindividual variability of multilead ECG recordings," *IEEE Transactions on Biomedical Engineering*, vol. 48, no. 5, pp. 551–559, 2001.

[9] B. P. Simon and C. Eswaran, "An ECG classifier designed using modified decision based neural networks," *Computers and Biomedical Research*, vol. 30, no. 4, pp. 257–272, 1997.

[10] G. Wuebbeler, et al., "Human verification by heart beat signals," Working Group 8.42, Physikalisch-Technische Bundesanstalt (PTB), Berlin, Germany, 2004, http://www.berlin.ptb.de/8/84/842/BIOMETRIE/842biometriee.html.

[11] M. Oeff, H. Koch, R. Bousseljot, and D. Kreiseler, "The PTB Diagnostic ECG Database," National Metrology Institute of Germany, http://www.physionet.org/physiobank/database/ptbdb/.

[12] The MIT-BIH Normal Sinus Rhythm Database, http://www.physionet.org/physiobank/database/nsrdb/.

[13] L. Sörnmo and P. Laguna, *Bioelectrical Signal Processing in Cardiac and Neurological Applications*, Elsevier, Amsterdam, The Netherlands, 2005.

[14] J. P. Martínez, R. Almeida, S. Olmos, A. P. Rocha, and P. Laguna, "A wavelet-based ECG delineator: evaluation on standard databases," *IEEE Transactions on Biomedical Engineering*, vol. 51, no. 4, pp. 570–581, 2004.

[15] A. L. Goldberger, L. A. N. Amaral, L. Glass, et al., "PhysioBank, PhysioToolkit, and PhysioNet: components of a new research resource for complex physiologic signals," *Circulation*, vol. 101, no. 23, pp. e215–e220, 2000.

[16] P. Laguna, R. Jan, E. Bogatell, and D. V. Anglada, "QRS detection and waveform boundary recognition using ecgpuwave," http://www.physionet.org/physiotools/ecgpuwave, 2002.

[17] Y. Wang, K. N. Plataniotis, and D. Hatzinakos, "Integrating analytic and appearance attributes for human identification from ECG signal," in *Proceedings of Biometrics Symposiums (BSYM '06)*, Baltimore, Md, USA, September 2006.

[18] J. Lu, *Discriminant learning for face recognition*, Ph.D. thesis, University of Toronto, Toronto, Ontario, Canada, 2004.

[19] K. N. Plataniotis, D. Hatzinakos, and J. K. M. Lee, "ECG biometric recognition without fiducial detection," in *Proceedings of Biometrics Symposiums (BSYM '06)*, Baltimore, Md, USA, September 2006.

[20] K. Grauer, *A Practical Guide to ECG Interpretation*, Elsevier Health Sciences, Oxford, UK, 1998.